World Journal of Engineering and Technology, 2024, 12, 976-986
https://www.scirp.org/journal/wjet
ISSN Online: 2331-4249
ISSN Print: 2331-4222

Analysis of the Flow of a Molten Slag in an Open Channel Using Transient and Steady-State Solutions of the Saint-Venant Equations

Miguel A. Barron, Joan Reyes, Aristeo Garrido

Departamento de Materiales, Universidad Autonoma Metropolitana Azcapotzalco, Ciudad de Mexico, Mexico
Email: bmma@azc.uam.mx

How to cite this paper: Barron, M.A., Reyes, J. and Garrido, A. (2024) Analysis of the Flow of a Molten Slag in an Open Channel Using Transient and Steady-State Solutions of the Saint-Venant Equations. *World Journal of Engineering and Technology*, **12**, 976-986.
https://doi.org/10.4236/wjet.2024.124060

Received: October 10, 2024
Accepted: November 3, 2024
Published: November 6, 2024

Abstract

In recent years, metallurgical slags have been increasingly used as materials for the manufacture of cement, pavement and filling material. The transport of the molten slag to the receiving pots is carried out through open channels. The transient and steady-state flow of a molten slag in a rectangular open channel is numerically analyzed here. For the transient flow, the Saint-Venant equations were numerically solved. For the steady-state flow, the derivatives in time and space in the Saint-Venant equations were set equal to zero and a polynomial of degree 3 is obtained whose roots are the slag height values. It was assumed that the viscosity of the slag has an Arrhenius-type behavior with temperature. Four values of temperature values, namely 1723.15, 1773.15, 1823.15, 18873.15 ˚K, and five values of the angle of inclination of the channel, namely 1, 2, 3, 4, 5 degrees, are considered. Numerical results show that the steady-state values of the height and velocity of the molten slag depend strongly on the temperature of the slag and the angle of inclination of the channel. As the slag temperature and channel angle increase, the value of the steady-state slag height decreases. The value of the steady-state slag velocity increases as the slag temperature and channel inclination angle increase.

Keywords

Molten Slag, Open Channel, Phase-Portrait, Saint-Venant Equations, Steady State, Transient Solution

1. Introduction

The flow of molten slag in open channels is interesting from both an academic and an industrial point of view. The open channels for the metallurgical industry are very different from those used for water transportation. The former are short in length so that the molten metal or slag does not solidify or reoxidize; They have a steeper slope, and the material from which they are made must withstand the high temperatures of the molten material without degrading. Works on the flow of water in open channels have been published for many decades, however, literature on the transport of molten slag in the metallurgical field is still scarce. In [1], it was studied the fluid flow in the blast furnace trough using both physical model and commercial fluid flow software. In [2], the flow characteristics in the taphole region of a blast furnace trough was analyzed using a 1/5th scale perspex model. Besides, velocities and turbulence intensities were measured by means of laser doppler velocimetry (LDV). In [3], the transient three-dimensional turbulent flow in a blast furnace trough was studied using Computational Fluid Dynamics software (CFD). The effect of blast furnace trough geometry on the slag-metal separation was analyzed using CFD numerical simulation in [4]. In [5], a transient 3D CFD model was solved to investigate the features of the multiphase flow in a blast furnace trough. Most of these works perform complex three-dimensional transient numerical simulations using Computational Fluid Dynamics tools. The results of these simulations, given that they resolve particular cases in great detail, are difficult to generalize to understand the basic aspects of fluid flow of molten slag in open channels.

The flow of molten slag in an open channel is three-dimensional and turbulent in nature. In addition, heat flow and phase changes make the analysis more complicated. However, the Saint-Venant equations are still used to properly describe the one-dimensional flow of liquids in channels under the following conditions: the slope of the channel is relatively small and without abrupt changes, the cross section is uniform, the channel is straight, the pressure distribution is hydrostatic, and the speed is uniform [6]. In a recent work [7], the present authors studied the unsteady, non-uniform flow of a molten blast furnace slag in a rectangular open channel through the numerical solution of the Saint-Venant equations. They conclude that, for the temperatures considered, the slag flow in the channel for an angle of 5 degrees is supercritical in nature. However, for an angle of 1 degree the flow is transcritical, that is, it presents a transition from subcritical to supercritical. In this work, the flow of a molten blast furnace slag in a rectangular open channel using transient and stable solutions of the Saint-Venant equations is studied. The effect of the angle of inclination of the open channel and the temperature of the slag on the transient behavior of the height and velocity is analyzed through the numerical solution of the Saint-Venant equations. It is assumed that the viscosity of the slag has an Arrhenius-type behavior with temperature. Saint-Venant equations are solved using an explicit backwards finite difference scheme. Furthermore, the equilibrium points, or steady-state solutions, of the Saint-Venant equations are analytically obtained, finding the roots of a polynomial of third degree obtained. A phase portrait of the flow was constructed from different initial conditions that show the convergence and stability of the steady-state values.

2. The Saint-Venant Equations

These equations consist of a continuity equation and momentum equations that account for gravitational forces and friction [6]. They are derived assuming shallow water conditions, which means that the depth of the liquid is small compared to the horizontal dimension of the flows. The Saint-Venant equations are expressed by the following equations:

Continuity equation:

$$b\frac{\partial h}{\partial t}+\frac{\partial Q}{\partial x}=0 \tag{1}$$

Momentum equation:

$$\frac{\partial Q}{\partial t}+\frac{1}{b}\frac{\partial}{\partial x}\left(\frac{Q^2}{h}\right)+gbh\left(\frac{\partial h}{\partial x}+S_f-S_0\right)=0 \tag{2}$$

In the above equations, h and Q are the height of the liquid and the volumetric flow rate, respectively, t is time and x is the space coordinate. Besides, b is the width of the channel, g is the gravitational acceleration, $S_0=\tan(\theta)$ is the channel slope, θ is the inclination angle of the channel, and S_f is the friction slope which can be estimated from the Darcy-Weisbach formula [8]:

$$S_f=f_D\frac{u^2}{8gh} \tag{3}$$

where f_D is the frictional resistance coefficient and u is the liquid velocity. The value of f_D depends on the type of flow [8]:

$$f_D=\frac{C}{Re}\quad \text{for laminar flow} \tag{4}$$

$$f_D=\frac{0.223}{Re^{0.25}}\quad \text{for transition flow} \tag{5}$$

$$f_D=\left[2\log\left(\frac{2h}{e_r}\right)+1.74\right]^{-2}\quad \text{for turbulent flow} \tag{6}$$

C is a constant, Re is the Reynolds number, and e_r is the rugosity of the wall channel. Re is defined as follows:

$$Re=\frac{D_h u\rho}{\mu} \tag{7}$$

In which D_h is the hydraulic diameter, and ρ and μ are the density and the viscosity of the liquid, respectively. D_h is defined as

$$D_h=\frac{4bh}{b+2h} \tag{8}$$

In order to introduce the effect of viscosity and temperature of the liquid in the Saint-Venant equations, the velocity u is solved from Equation (7) and substituted into Equation (3):

$$S_f=\frac{f_D}{8gh}\left(\frac{Re\mu}{D_h\rho}\right)^2 \tag{9}$$

Since viscosity is a function of temperature, this variable is considered implicitly in the solution of the Saint-Venant equations.

3. Steady-State Solutions of the Saint-Venant Equations

The steady-state solutions of the Saint-Venant equations are obtained by setting the time and space derivatives in Equations (1-2) to zero. This implies that

$$S_f - S_0 = 0 \tag{10}$$

By algebraically manipulating Equations (8-10) it is obtained the following expression for the steady-state value of h, namely h_s:

$$\frac{b^2 h_s^3}{\left(b+2h_s\right)^2} - \frac{f_D}{128 g S_0}\left(\frac{Re\mu}{\rho}\right)^2 = 0 \tag{11}$$

Expanding and regrouping terms in the previous equation, one obtains a polynomial of degree 3 for h_s:

$$A_1 h_s^3 + A_2 h_s^2 + A_3 h_s + A_4 = 0 \tag{12}$$

where

$$A_1 = b^2 \tag{13}$$

$$A_2 = -4K \tag{14}$$

$$A_3 = -4bK \tag{15}$$

$$A_4 = -b^2 K \tag{16}$$

$$K = \frac{f_D}{128 g S_0}\left(\frac{Re\mu}{\rho}\right)^2 \tag{17}$$

The values of the liquid velocity in steady state corresponding to the values of h_s are obtained in this way:

$$u_s = \frac{Q_0}{b h_s} \tag{18}$$

The Froude numbers are calculated using the steady-state values of height and velocity through the expression

$$Fr = \frac{u_s}{\sqrt{g h_s}} \tag{19}$$

For $Fr < 1$ the flow regime is subcritical, gravitational forces are dominant and the flow has large depths and small velocities. For $Fr > 1$ the flow regime is supercritical, the inertial forces are dominant and the flow has small depths and large velocities [9]. For $Fr = 1$ the flow regime is critical and gravity waves may arise. The critical depth h_c is the flow depth at a section of the channel where the flow is critical. It is calculated in this way [10]:

$$h_c = \left(\frac{Q_0^2}{b^2 g}\right)^{1/3} \tag{20}$$

and the critical velocity is given by

$$u_c = \sqrt{gh_c} \tag{21}$$

4. Numerical Solution of the Saint-Venant Equations

Saint-Venant equations (1)-(2) are numerically solved using an explicit backwards finite difference scheme [11] [12]. Initial conditions and boundary conditions for h and Q are considered as follows:
Initial conditions for h and Q:

$$h(0,x) = h_0 \tag{22}$$

$$Q(0,x) = Q_0 \tag{23}$$

Boundary condition for h:

$$h(t,0) = h_0 \tag{24}$$

Boundary condition for Q: a half-sinusoidal perturbation pulse with amplitude A, period T and duration t_p is imposed at the inlet of the channel to analyze the transient response [11]:

$$Q(t,0) = Q_0 + A\sin\left(\frac{2\pi t}{T}\right), t \le t_p \tag{25}$$

$$Q(t,0) = Q_0, t > t_p \tag{26}$$

where Q_0 = 0.038 m^3/s, $A = 0.75Q_0$, T = 5 s and t_p = 5 s.

Parameters of the rectangular open channel considered in the numerical simulation are shown in **Table 1** [13].

Table 1. Open channel parameters [13].

Parameter	Value
Initial height (h_0)	0.15 m
Volumetric flow rate (Q_0)	0.038 m^3/s
Channel width (b)	0.20 m
Initial velocity (u_0)	1.2667 m/s
Channel length (L)	10.0 m
Inclination angle (θ)	5 degrees
Initial velocity (u_0)	1.27 m/s

The discretized Saint-Venant equations are solved for a simulation time of 20 s, with setting C = 24 and $Re = 4 \times 10^3$. A channel length of 10 m is assumed and 500 nodes were employed with Δx = 0.02 m. A time step $\Delta t = 1 \times 10^{-3}$ s is established [11].

5. Results and Comments

Five values of the channel inclination angle are considered in the numerical simulations, namely 1, 2, 3, 4 and 5 degrees. As in [11], four temperature values are assumed: 1450˚C, 1500˚C, 1550˚C, and 1600˚C, corresponding to 1723.15, 1773.15, 1823.15, and 1873.15 ˚K, respectively. For the numerical simulations, a molten blast furnace slag is considered, the physical properties of which are described in [14]. An Arrhenius-type dependence of the viscosity with temperature is assumed:

$$\mu = \mu_0 \exp\left(\frac{Ea}{RT}\right) \tag{27}$$

Above μ_0 is the pre-exponential factor, Ea is the activation energy, R is the gas constant, and T is the absolute temperature (˚K). Viscosity parameters shown in **Table 2** are taken from [14].

Table 2. Viscosity parameters of the blast furnace slag, taken from [14].

Parameter	Value
μ_0, kg/(m.s)	9.469×10^{-5}
Ea, J/mol	1.940×10^{5}

Table 3 shows the Froude numbers for the different combinations of temperature and inclination angle of the channel.

Table 3. Froude numbers.

T (˚K)	$\theta = 1^\circ$	$\theta = 2^\circ$	$\theta = 3^\circ$	$\theta = 4^\circ$	$\theta = 5^\circ$
1723.15	1.62518	2.71534	3.59150	4.35770	5.04688
1773.15	2.85603	4.57268	5.93154	7.11095	8.16503
1823.15	4.62335	7.24903	9.28030	11.02499	12.58445
1873.15	6.86626	10.93795	13.91215	16.43151	18.67344

During the numerical simulations, the height, velocity and volumetric flow rate of the molten slag at the channel discharge were monitored. The results are depicted in **Figures 1**, **Figures 2** and **Figures 3**, in which h_c = 0.1544 m and u_c = 1.2306 m/s. **Figure 1** shows that for channel inclination angles of 1, 2 and 3 degrees and T = 1723.15 ˚K the slag height shows transient peaks, due to the half-sinusoidal pulse, above the critical height. Subsequently, the height decreases below the critical height of its steady-state value. For all channel inclination angles considered, **Figure 1** shows that the steady-state slag height is less than the critical height, represented by the dashed line. Furthermore, according to **Table 3**, the value of the Froude number is always greater than unity for all possible combinations of angles and temperatures.

Figure 2 shows the dynamic behavior of the slag velocity for $T = 1723.15$ ˚K which, after transient peaks, finally reaches its steady-state value above the critical value shown in the dashed line. The above means that, in any case, the flow is considered supercritical in nature.

The time evolution of the volumetric flow rate for $T = 1723.15$ K and different channel angles at the channel discharge are shown in Figure 3. The transient peaks that appear are due to the half-sinusoidal pulse imposed as a boundary condition at the channel input. This pulse has a duration of 5 s, so after this time, the volumetric flow values return to their original value Q_0.

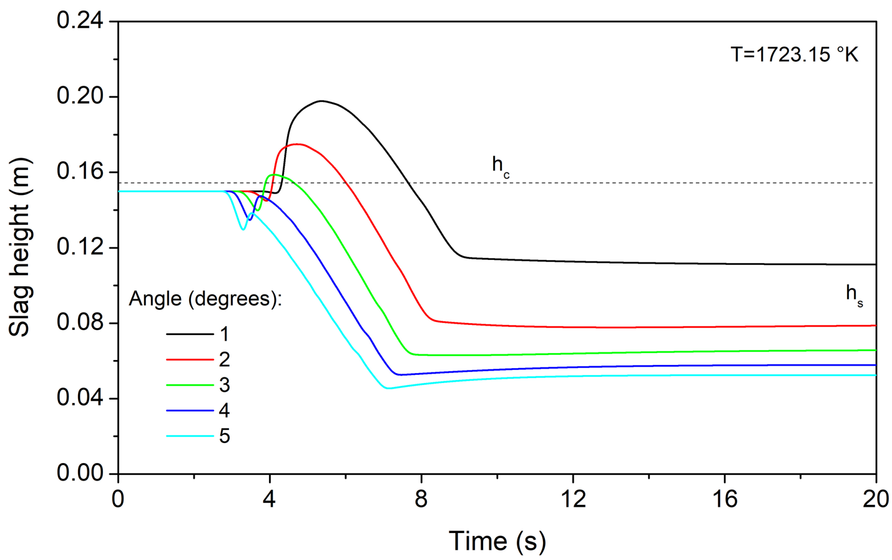

Figure 1. Transient behavior of the slag height at the channel discharge for different values of the channel inclination angle at $T = 1723.15$ ˚K.

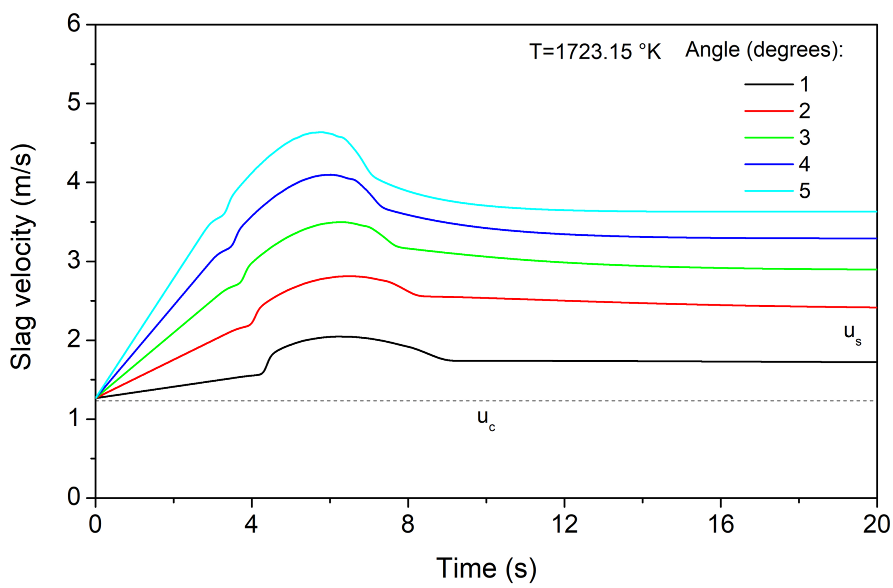

Figure 2. Transient behavior of the slag velocity at the channel discharge for different values of the channel inclination angle at $T = 1723.15$ ˚K.

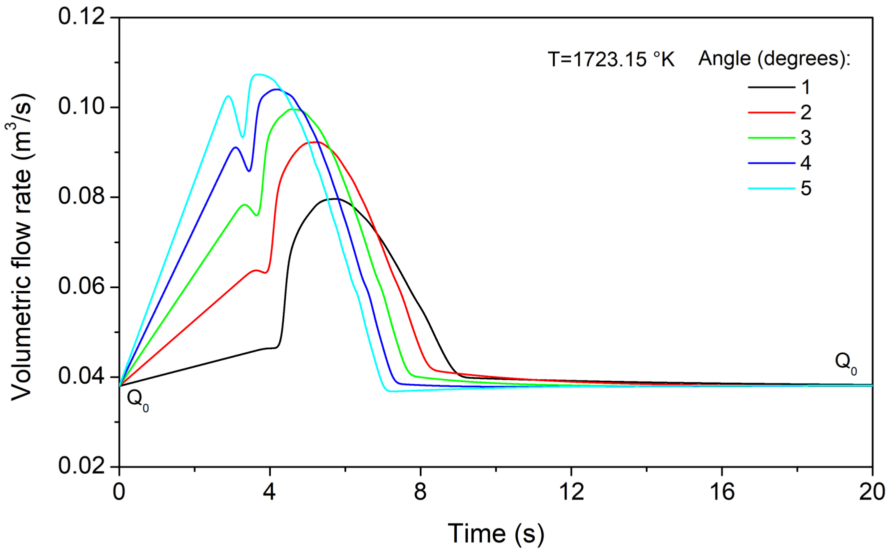

Figure 3. Transient behavior of the slag volumetric flow rate at the channel discharge for different values of the channel inclination angle at T = 1723.15 ˚K.

The polynomial given by Equation (12) has one real root and two imaginary roots. For example, for $\theta = 5$ degrees, T = 1723.15 ˚K, $\mu = 0.72$ kg/(m.s), $\rho = 2700$ kg/m^3, $Re = 4000$ and $f_D = 24/\text{Re}$, the corresponding polynomial has the following roots: i) 0.0525, ii) −0.0231 + 0.0255i, iii) −0.0231 − 0.0255i. **Table 4** shows the steady-state values of the molten slag height corresponding to the real values of the polynomial roots.

Table 4. Steady-state molten slag heights (m).

T (˚K)	θ = 1˚	θ = 2˚	θ = 3˚	θ = 4˚	θ = 5˚
1723.15	0.11179	0.07944	0.06583	0.05787	0.05247
1773.15	0.07686	0.05613	0.04712	0.04176	0.03808
1823.15	0.05544	0.04128	0.03498	0.03117	0.02854
1873.15	0.04146	0.03130	0.02670	0.02389	0.02194

Figure 4 shows the steady-state slag height as a function of temperature for different inclination angles of the open channel. It can be seen that as the temperature increases, the steady-state value of the slag height decreases. The same inverse dependence is noted with the angle of inclination: as the channel increases its inclination, the stable height of the slag decreases. The opposite occurs with the velocity of the slag, as is seen in **Figure 5**: As the temperature and the angle of inclination increase, the velocity in the steady state increases. This may be due to two factors: i) As the temperature increases, the viscosity of the slag decreases, which in turn decreases the resistance to flow, and ii) as the angle of inclination of the channel increases, the vertical component of the

gravitational acceleration is increased, and consequently the slag velocity is also increased.

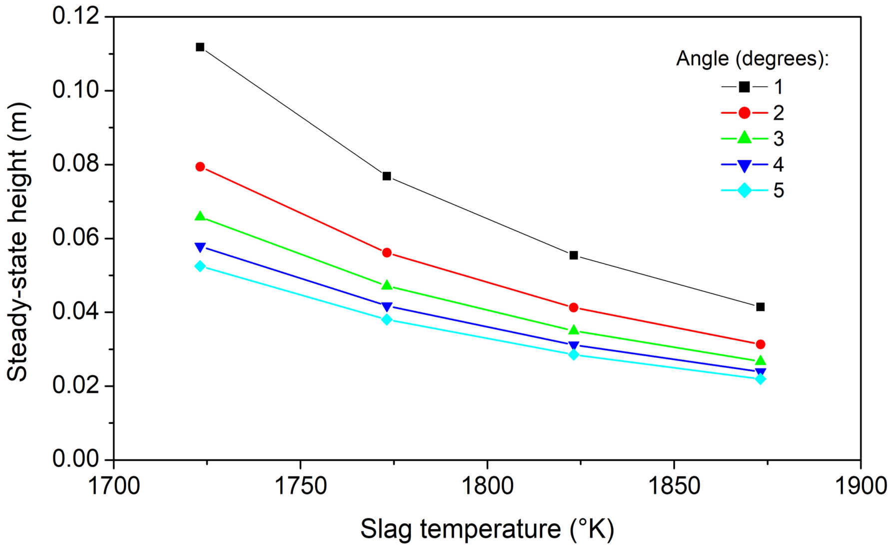

Figure 4. Steady-state height as a function of slag temperature for different channel inclination angles.

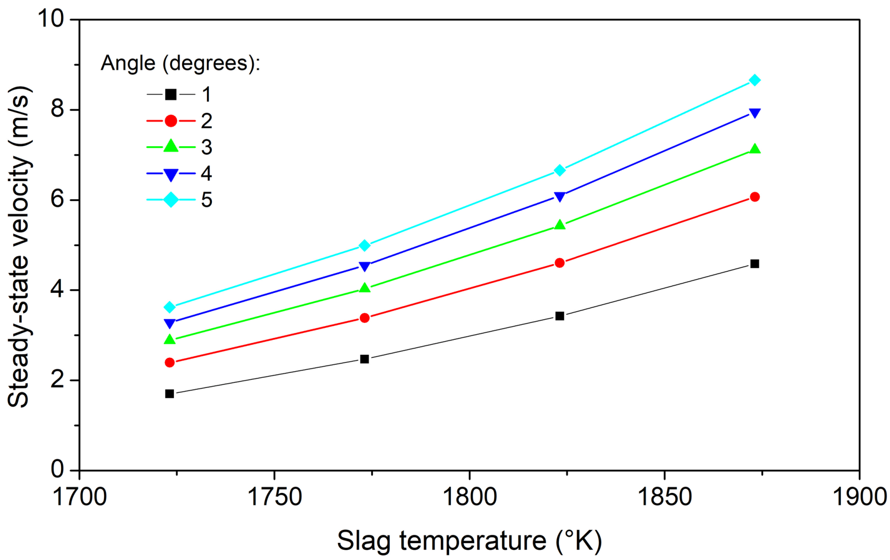

Figure 5. Steady-state velocity as a function of slag temperature for different channel inclination angles.

Finally, numerical simulations were carried out using different initial conditions in height and velocity, keeping the temperature constant at 1723.15 ˚K and the channel inclination angle at 1 degree. The results are shown in the form of a phase portrait in **Figure 6**, where the convergence of all trajectories towards the corresponding steady state can be seen. This steady state, in which $h_s = 0.111$ m and its corresponding $u_s = 0.038/(0.2 \times 0.11) = 1.712$ m/s, coincides with that reported in **Table 4**.

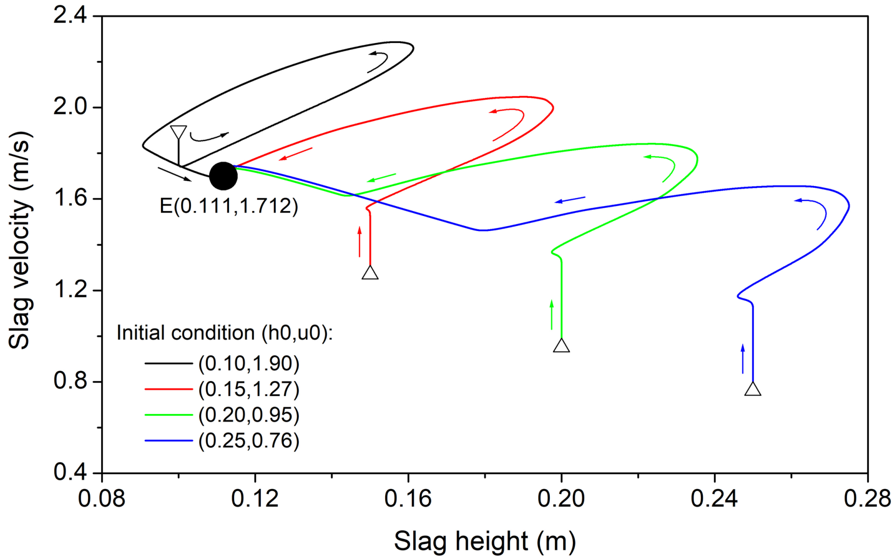

Figure 6. Phase-portrait of the flow for a temperature of 1725.15 ˚K and a channel angle of 1 degree.

6. Conclusions

The transient and steady-state flow of a molten slag in an open channel is numerically analyzed. For the transient flow a half-sinusoidal pulse on the volumetric flow rate is imposed as a boundary condition at the channel input and the Saint-Venant equations were solved numerically. For the steady-state flow, the derivatives in time and space in the Saint-Venant equations were set equal to zero, and a polynomial of degree 3, whose roots are the slag height values, was obtained. It was assumed that the viscosity of the slag has an Arrhenius-type behavior with temperature. Four values of temperature and five values of the angle of inclination of the channel are considered. Based on the numerical results obtained, the following conclusions emerge:

The time trajectories of the height and velocity of the slag present temporary peaks due to the half-sinusoidal pulse imposed at the channel entrance, but subsequently reach a steady state value. The steady-state values of the height and velocity of the molten slag depend strongly on the temperature of the slag and the angle of inclination of the channel. As the slag temperature and channel angle increase, the value of the steady-state slag height decreases. The value of the steady-state slag velocity increases as the slag temperature and channel inclination angle increase. Finally, a phase portrait of the flow shows the convergence of different initial conditions towards the corresponding steady state in the range of values considered.

The results reported in this work are limited to the one-dimensional analysis of the flow of a molten slag in a rectangular channel under the influence of only two variables, namely the angle of inclination of the channel and the temperature of the slag. Further work should include additional variables such as different channel geometries, higher Reynolds numbers and slag density. The results shown in this work, since they are numerical in nature, should be verified through experimental data.

Conflicts of Interest

The authors declare no conflicts of interest regarding the publication of this paper.

References

[1] Luomala, M.J., Paananen, T.T., Köykkä, M.J., Juhani Fabritius, T.M., Nevala, H. and Härkki, J.J. (2001) Modelling of Fluid Flows in the Blast Furnace Trough. *Steel Research*, **72**, 130-135. https://doi.org/10.1002/srin.200100096

[2] He, Q., Evans, G., Zulli, P., Tanzil, F. and Lee, B. (2002) Flow Characteristics in a Blast Furnace Trough. *ISIJ International*, **42**, 844-851. https://doi.org/10.2355/isijinternational.42.844

[3] Wang, L., Pan, C. and Cheng, W. (2017) Numerical Analysis on Flow Behavior of Molten Iron and Slag in Main Trough of Blast Furnace during Tapping Process. *Advances in Numerical Analysis*, **2017**, Article ID: 6713160. https://doi.org/10.1155/2017/6713160

[4] Kou, M., Yao, S., Wu, S., Zhou, H. and Xu, J. (2018) Effects of Blast Furnace Main Trough Geometry on the Slag-Metal Separation Based on Numerical Simulation. *Steel Research International*, **90**, Article ID: 1800383. https://doi.org/10.1002/srin.201800383

[5] Barral, P., Pérez-Pérez, L.J. and Quintela, P. (2023) Transient 3D Hydrodynamic Model of a Blast Furnace Main Trough. *Engineering Applications of Computational Fluid Mechanics*, **17**, Article ID: 2280776. https://doi.org/10.1080/19942060.2023.2280776

[6] Chaudhry, M.H. (2008) Open-Channel Flow. Second Edition, Springer. https://doi.org/10.1007/978-0-387-68648-6

[7] Barron, M.A., Reyes, J., Garrido, A. (2024) Numerical Simulation of the Flow of a Molten Blast Furnace Slag in an Open Channel. *World Journal of Engineering and Technology*, **12**, 963-975.

[8] Zhang, H., Zhang, F., Shen, K. and Yuan, M. (2015) A Surface and Subsurface Model for the Simulation of Rainfall Infiltration in Slopes. *IOP Conference Series: Earth and Environmental Science*, **26**, Article ID: 012025. https://doi.org/10.1088/1755-1315/26/1/012025

[9] Sturm, T.W. (2021) Open Channel Hydraulics. Third Edition, McGraw-Hill.

[10] Osman-Akan, A. (2006) Open Channel Hydraulics. Butterworth-Heinemann.

[11] Barron, M.A., Reyes, J. and Miranda, D.Y. (2022) Unsteady Non-Uniform Flow of Molten Metals in Rectangular Open Channels. *World Journal of Engineering and Technology*, **10**, 593-604. https://doi.org/10.4236/wjet.2022.103038

[12] Keskin, M.E. and Ağiralioğlu, N. (1997) A Simplified Dynamic Model for Flood Routing in Rectangular Channels. *Journal of Hydrology*, **202**, 302-314. https://doi.org/10.1016/s0022-1694(97)00072-3

[13] Szekely, J. (1979) Fluid Flow Phenomena in Metals Processing. Academic Press.

[14] Chen, M., Zhang, D., Kou, M. and Zhao, B. (2014) Viscosities of Iron Blast Furnace Slags. *ISIJ International*, **54**, 2025-2030. https://doi.org/10.2355/isijinternational.54.2025